GEOPHYSICS, VOL. 69, NO. 2 (MARCH-APRIL 2004); P. 466–471, 4 FIGS., 1 TABLE.
10.1190/1.1707066

Fast monostatic GPR modeling

Luca Baradello*, José M. Carcione*, and Davide Gei*

ABSTRACT

We propose the exploding-reflector method to simulate a monostatic survey with a single simulation. The exploding reflector, used in seismic modeling, is adapted for ground-penetrating radar (GPR) modeling by using the analogy between acoustic and electromagnetic waves. The method can be used with ray tracing to obtain the location of the interfaces and estimate the properties of the medium on the basis of the traveltimes and reflection amplitudes. In particular, these can provide a better estimation of the conductivity and geometrical details. The modeling methodology is complemented with the use of the plane-wave method. The technique is illustrated with GPR data from an excavated tomb of the nineteenth century.

INTRODUCTION

Ground penetrating radar (GPR) is a useful tool in archeological investigations, in particular for locating graves and tombs. Archeological applications include the work by Imai et al. (1987), who conducted GPR and resistivity surveys to locate ancient Japanese dwellings, burial mounds, and a distribution of significant "cultural" strata. Other applications include the search for buried remains of a sixteenth-century Basque whaling station on the Labrador coast (Vaughn, 1986), the discovery of Roman foundations in Britain (Stove and Addyman, 1989), and the search for graves in cemeteries and churches (Bevan, 1991). Recently, Sternberg and McGill (1995) conducted successful GPR surveys in archaeological areas of southern Arizona. Integration of GPR measurements with seismic surveys has been applied by Brizzolari et al. (1992) to an archeological site near Rome. More recently, Pipan et al. (1999) acquired 3D multifold data at the Aquileia archeological park (northern Italy), Pérez Gracia et al. (2000) used the technique to locate ancient graves at the cathedral of Valencia (Spain), and GPR surveys have been conducted at Qumran (Israel) to locate graves from the first century AD (Jol et al., 2002).

Archeological targets can be geometrically complex, and modeling is needed to interpret the GPR response from these targets. A drawback is that the simulation of a monostatic survey requires several computations, one for each trace. To overcome this problem, we propose the use of the exploding-reflector and plane-wave methods, which approximate a monostatic survey with a single simulation. The plane-wave method has a simple implementation. It consists in propagating a horizontal, localized plane-wave front down from the surface and recording the response of the subsurface model at the surface.

Our main objective is to develop the exploding-reflector concept for GPR modeling using the analogy between acoustic and electromagnetic waves (Carcione and Cavallini, 1995). The exploding-reflector method has been used in seismic applications to approximate zero-offset stacked sections (Baysal et al., 1984; Carcione et al., 1994) without physical multiple reflections, which are, in principle, absent from those sections and constitute unwanted artifacts in migration processes (Baysal et al., 1983). The computation of synthetic seismograms requires the use of the exploding-reflector concept (Loewenthal et al., 1976) and the so-called nonreflecting wave equation (Baysal et al., 1984). Each reflection point in the subsurface explodes at $t = 0$ with a magnitude proportional to the normal incidence reflection coefficient. Moreover, the source strength is multiplied by the average transmission losses and divided by the geometrical-spreading factor. Note that these corrections are not applied for the simulation of zero-offset stacked sections, but they are required when approximating monostatic surveys. Since the source is located at the interface, the traveltime will be half the physical traveltime. Therefore, the phase velocities are halved to obtain the correct two-way traveltime. Due to sampling constraints, halving the velocities implies doubling the number of grid points. Therefore, the method is less efficient than the plane-wave approach. The fact that the sources are located on the interfaces generates nonphysical multiple reflections. To avoid these reflections, the wave equation is modified to model a constant impedance medium over the whole model space (i.e., the nonreflecting wave equation mentioned above). In this way, the recorded events are primary energy. The method generates normal-incidence reflections (i.e., those

Manuscript received by the Editor November 11, 2002; revised manuscript received July 14, 2003.
*Istituto Nazionale di Oceanografia e di Geofisica Sperimentale, Borgo Grotta Gigante 42c, 34010 Sgonico, Trieste, Italy. E-mail: lbardello@ogs.trieste.it; jcarcione@ogs.trieste.it; dgei@ogs.trieste.it.

having identical downgoing and upgoing wave paths). Note that the amplitudes are approximate but the traveltimes are correct because Snell's law depends on the wave velocity and not on the impedance. Therefore, the angle of refraction at the interfaces is that predicted by Snell's law.

In the seismic case, density is used as a free parameter to obtain a constant impedance model and avoid multiple reflections. Density is mathematically analogous to the magnetic permeability for the electromagnetic case (Carcione and Cavallini, 1995). We scale this property to obtain a model where all the media have the same electromagnetic impedance. The condition that the phase velocity remains unchanged in a particular material also requires that the permittivity and the conductivity be scaled proportionally.

We propose the following methodology for the interpretation of monostatic surveys, which requires the knowledge of either the electromagnetic velocity of the ground or the geometrical features of the target. The velocity can be obtained from stratigraphic studies of previous excavations and bistatic single common-midpoint experiments. A preliminary model is obtained with a ray-tracing algorithm by locating the interfaces on the basis of the traveltimes. However, the ray tracing requires smooth interfaces (zero-radius features such as corners cannot be modeled), and the corresponding reflection amplitudes are not correct. Hence, we perform exploding-reflector and plane-wave experiments to refine the model and better estimate the geometrical features and the conductivity on the basis of the reflection amplitudes. This forward approach is an alternative and complementary methodology to inversion methods that estimate permittivity using monostatic data (e.g., Spagnolini, 1997).

In the next section, we develop the exploding-reflector concept for electromagnetic fields. Next, we apply the modeling methodology developed here to GPR data from an excavated tomb of the nineteenth century.

THE EXPLODING-REFLECTOR METHOD FOR GPR MODELING

We illustrate our approach with the ray paths for the plane-wave and exploding-reflector simulations shown in Figure 1. The plane-wave experiment sums the response of many receiver antennas with only one transmitter, but the traveltimes obtained with this method are not those of the monostatic survey. A simple example is given by a single diffraction point

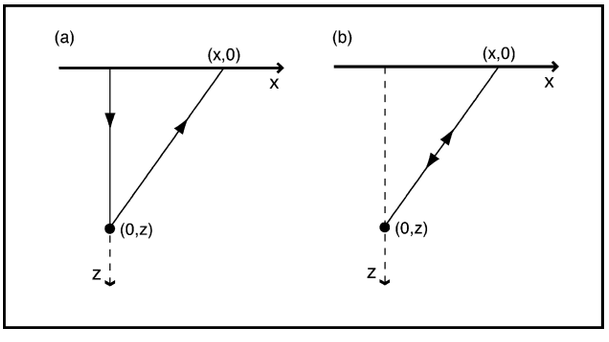

Figure 1. The raypaths for the plane-wave (a) and exploding-reflector (b) simulations.

at $(0, z)$. If v is the phase velocity of the medium, the traveltime at offset $(x, 0)$ is $t = z/v + \sqrt{x^2 + z^2}/v$, whereas a source and a receiver at $(x, 0)$ imply a traveltime $t = 2\sqrt{x^2 + z^2}/v$ (the method is also approximate for dipping layers). The plane-wave method yields more realistic amplitudes (including multiple reflections) than the exploding-reflector method, whereas the latter yields the same arrival times of the monostatic survey, but does not contain multiple reflections.

We assume propagation in the (x, z)-plane, and that the material properties and source characteristics are constant with respect to the y-coordinate. Implementation of the exploding-reflector method in GPR modeling implies the following. (1) A source is placed at every point on the interface. (2) The phase velocity of each medium is halved, to obtain the correct two-way traveltime for every diffraction and reflection event. (3) The source strength is proportional to the normal-incidence reflection coefficient and the transmission factor of the overlying layers, and inversely proportional to the geometrical-spreading factor at each point on the interface (a zero-offset raypath is normal to the reflecting interface). (4) We require that the electromagnetic impedance be the same for all media. Because the algorithm generates nonphysical events (the downgoing waves) and approximates a zero-offset stacked section, we must avoid multiple reflections.

We meet requirements (1)–(4) as follows.

1) The algorithm used here solves the electromagnetic equations in the time domain, and it is based on a grid method for computing the spatial derivatives. This implies a discretization of the model space. Then, at every grid point of each interface, a source with the same time history is initiated at time $t = 0$.
2) The phase velocity is given by

$$v_p = \left[\Re\left(\frac{1}{v_c}\right)\right]^{-1}, \tag{1}$$

where $\Re$ is the real-part operator, and

$$v_c = \frac{1}{\sqrt{\mu_0 \epsilon^*}} \tag{2}$$

is the complex velocity (Carcione, 1996a, b). We halve the phase velocity by the following substitution:

$$\mu_0 \rightarrow 4\mu_0. \tag{3}$$

Since the attenuation factor is $\alpha = -\omega\Im(1/v_c)$ (Carcione, 1996a, b), where $\Im$ is the imaginary-part operator, equation (3) ensures that the amplitude decay related to intrinsic attenuation corresponds to that of the two-way travel path.
3) The normal-incidence reflection coefficient between medium 1 and medium 2 is given by

$$R = \frac{I_2 - I_1}{I_2 + I_1}, \tag{4}$$

where we define the electromagnetic impedance $I = \mu_0 v_p$, in terms of the phase velocity. Actually, the complex velocity should be used in lossy media (Chew, 1990, p. 48), but the above definition avoids the use of complex quantities and provides the correct phase angle in the lossless case. Equation (4) is valid for the electric field of transverse-electric (TE) or transverse-magnetic

(TM) waves. The corresponding normal-incidence reflection coefficient for the magnetic field of the TE or TM waves has the opposite sign. The source strength should be proportional to R. Since R depends on the frequency ω, this requirement cannot be satisfied for all frequencies when using a time-domain solver. In this case, we consider the source strength to be proportional to $R(\omega_d)$, where ω_d is the dominant frequency of the source.

The transmission factor of the overlying layers is approximately given by

$$\bar{T} = \prod_i \left(1 - |R_i|^2\right), \tag{5}$$

where R_i is the normal-incidence reflection coefficient of the overlying layers (defined in terms of the complex velocity), and the product considers the transmission losses of the raypath going down and up. In addition, the source strength is inversely proportional to the geometrical-spreading factor (Neumann, 1973)

$$g = \sqrt{\frac{2}{v_{p1}} \sum_i h_i v_{pi}}, \tag{6}$$

where h_i and v_{pi} are the thickness and phase velocity of the overlying layers. The square root is due to the cylindrical divergence of 2D propagation.

4) We can avoid normal-incidence multiple reflections if all the media have the same electromagnetic impedance. This is evident from equation (4). In order to do this, we must scale all the material properties accordingly, that is, substitute μ_0, ϵ, and σ by new properties $\tilde{\mu}$, $\tilde{\epsilon}$, and $\tilde{\sigma}$. The complex impedance could be made constant by using the perfectly matched layer (PML) method introduced by Berenguer (1994) (i.e., using a complex magnetic permeability). However, although the PML method gives a constant impedance medium, the complex velocity is not that of equation (2) and, therefore, the location of the reflection events will not be correct. Since the aim of the exploding-reflector concept is to model the correct traveltimes of the primary events, we use a real magnetic permeability and try to minimize as much as possible the amplitude of the multiple reflections. This can be done by imposing the same "instantaneous" (optical) impedance for all the media. The instantaneous impedance is defined as $I^\infty = I(\omega = \infty)$, which corresponds to the "unrelaxed" (optical) response of the medium ($t = 0$). In this limit, $\sigma/\omega \to 0$, in general. Then, we assume

$$I^\infty = \sqrt{\frac{\tilde{\mu}}{\tilde{\epsilon}}} = k, \tag{7}$$

with k a real constant. Moreover, we must impose that the complex velocity (2) remains unchanged after introduction of the scaled properties, i.e.,

$$\mu_0 \epsilon^* = \tilde{\mu}\left(\tilde{\epsilon} - \frac{i}{\omega}\tilde{\sigma}\right). \tag{8}$$

This guarantees that the traveltime of the primary reflections events is correct. The choice

$$k = I_0 = \sqrt{\frac{\mu_0}{\epsilon_0}} \tag{9}$$

(the impedance of vacuum) implies

$$\tilde{\mu} = \frac{\mu_0}{a}, \quad \tilde{\epsilon} = a\epsilon, \quad \text{and} \quad \tilde{\sigma} = a\sigma, \tag{10}$$

where

$$a = \sqrt{\frac{\epsilon_0}{\epsilon}}. \tag{11}$$

Then, $I^\infty = I_0$, and equation (8) is satisfied.

The frequency- and time-domain electromagnetic equations are given in the Appendix. The radargrams are computed in the space-time domain.

SIMULATIONS

We used this methodology to obtain the response to a model of a ninteenth-century tomb found at the church of S. Nicolò of Belgrado di Varmo (Friuli-Venezia-Giulia, Italy). We identified the tomb in the church as shown in Figure 2. The data were acquired with a GSSI SIR 2000 control unit and a 400-MHz antenna unit. The trace window was 100 ns and digitized at 1024 samples per trace with a dynamic range of 16 bits. The spacing between adjacent traces is 5 cm. We acquired five parallel profiles each 1.8-m long and 0.5-m apart.

Using the methodology described in this paper, we obtained a model based on the geometrical characteristics of the tomb observed in the excavations. A vertical section of the model is shown in Figure 3, where the raypaths are displayed. The numbers correspond to materials whose properties are given in Table 1. The dielectric constants and conductivities are in good agreement with values reported by Stewart et al. (1994) and

Table 1. Electromagnetic properties.*

Medium	Description	ϵ (ϵ_0)	σ (S/m)
1	Cement	9	0.01
2	Gravel	8	0.1
3	Clayey soil	25	0.1
4	Tomb (brick)	9.5	0.1
5	Air	1	0
6	Water	80	0.01

*$\epsilon_0 = 8.85\ 10^{-12}$ F/m; $\mu_0 = 4\pi 10^{-7}$ H/m.

Figure 2. The nineteenth-century tomb (attributed to the priest Josepho Lotti) found at the church of S. Nicolò of Belgrado di Varmo (Friuli-Venezia-Giulia, Italy).

Daniels (1996). These values correspond to wet conditions (the weather was rainy before the survey). The interfaces used to trace the rays are shown as continuous and smooth lines going from one side to the other side of the model (smoothness of the interfaces is a requirement of the algorithm). The geometries obtained from the ray tracing coincide with the real features of the tomb.

The numerical mesh for both plane-wave and exploding reflector experiments has 225×225 grid points, with a grid spacing of 1 cm. The source is an horizontal electric current ($\mathcal{J}_y$), whose time history corresponds to that of the antenna measured in air, with a central frequency of nearly 400 MHz. To avoid wraparound, absorbing layers of length 30 grid points are implemented at the sides of the numerical mesh, with the upper absorbing layer located at the bottom of the mesh, because the Fourier differentiation is periodic. The Runge-Kutta method requires a time step of 0.01 ns.

Figure 4 shows the recorded data (a), the monostatic simulation (b), the plane-wave simulation (c) and the exploding-reflector simulation (d). The monostatic simulation consists of 33 numerical computations. The gain applied to the data and simulations is $-0.8 \log j + 0.03j + 2$, where j is the sample number. The reflection events have the following correspondence: (A) cement/gravel interface, (B) gravel/clayey soil interface, (C) clayey soil/brick interface, (D) brick/air interface, (E) air/water interface, and (F) clayey soil/brick interface (sides of the tomb). The exploding-reflector traveltimes are greater than the plane-wave traveltimes and coincide with those of the real radargram. The amplitude and phases of radargrams (a) and (d) are in good agreement. Differences between the exploding-reflector simulations and the real radargram can be due to scattering from inhomogeneities and to the presence of multiple reflections (see the reflection peaking at 11 ns) in the real radargram.

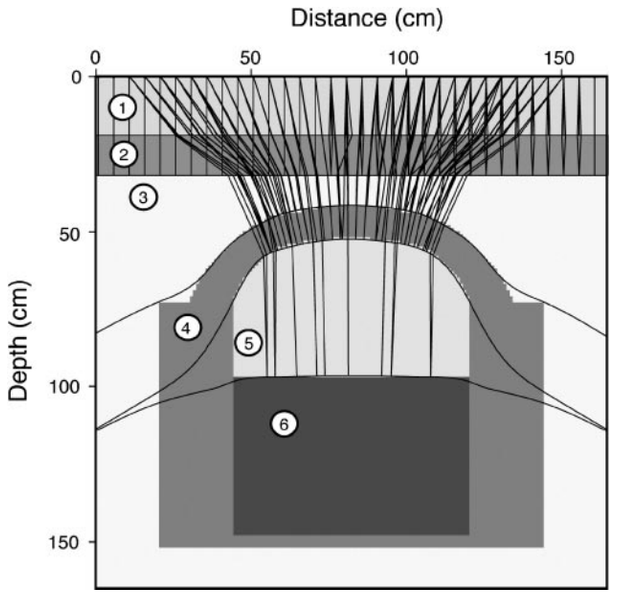

Figure 3. Cross-sectional representation of the excavation and modeled raypaths. The numbers correspond to materials whose properties are given in Table 1. The interfaces used to trace the rays are shown as continuous and smooth lines.

CONCLUSIONS

The exploding-reflector and plane-wave methods constitute a simple and efficient methodology for interpreting monostatic surveys. The exploding-reflector method provides the correct traveltimes of diffractions and reflections events, whereas the plane-wave method yields more realistic amplitudes and multiple reflections. A modification of the first method to include transmission losses and geometrical spreading make it more suitable for approximating monostatic surveys regarding the amplitudes. However, it is important to note that when the velocity variations are rapid in the horizontal direction, the exploding-reflector model may give incorrect results (this is the case when different rays cross each other on the way to the surface). These methods, aided by ray tracing, have been successfully used to analyze the radargram corresponding to a nineteenth-century tomb. This example shows that the methodology is effective in properly finding the geometrical features of the tomb. In this sense, this approach can be a useful tool for the interpretation of the GPR response of complex targets. A limitation is that a priori knowledge is required, either of the electromagnetic properties of the media or the geometrical features of the target. Monostatic surveys should then be complemented with wide-angle reflection profiles to estimate the electromagnetic velocities, and borehole logging can be useful to determine the soil conditions and properties. With regard to the exploding-reflector method, it is also useful to approximate stacked radargrams with a single calculation, and for migration algorithms, where it is necessary to avoid interlayer reverberations.

ACKNOWLEDGMENTS

We have used the ray tracing of SEISMIC UNIX. This work was financed in part by the European Union under the framework of the HYGEIA project. We are grateful to the associate editor and reviewers for useful comments.

APPENDIX A

TIME-DOMAIN TE EQUATIONS

Maxwell's equations for isotropic media and time harmonic fields with time dependence $\exp(i\omega t)$, where ω is the angular frequency, read:

$$\nabla \times \mathbf{E} = -i\omega\mu_0\mathbf{H} + \mathbf{M}$$
$$\nabla \times \mathbf{H} = i\omega\epsilon\mathbf{E} + \sigma\mathbf{E} + \mathbf{J}_s = i\omega\epsilon^*\mathbf{E} + \mathbf{J}_s, \quad \text{(A-1)}$$

where the symbol $\times$ denotes the vector product, $i = \sqrt{-1}$, $\mathbf{E}$ is the electric field, $\mathbf{H}$ is the magnetic field, $\mathbf{J}_s$ is any electric source, $\mathbf{M}$ is any magnetic source, μ_0 is the magnetic permeability of vacuum (appropriate for GPR applications), ϵ is the dielectric permittivity, σ is the conductivity, and

$$\epsilon^*(\omega) = \epsilon - \frac{i}{\omega}\sigma \quad \text{(A-2)}$$

is the complex permittivity (Chew, 1990). Equation (A-1) can then be combined to produce wave equations for both the transverse electric (TE) and the transverse magnetic (TM) fields. For GPR applications, we are interested in TE propagation.

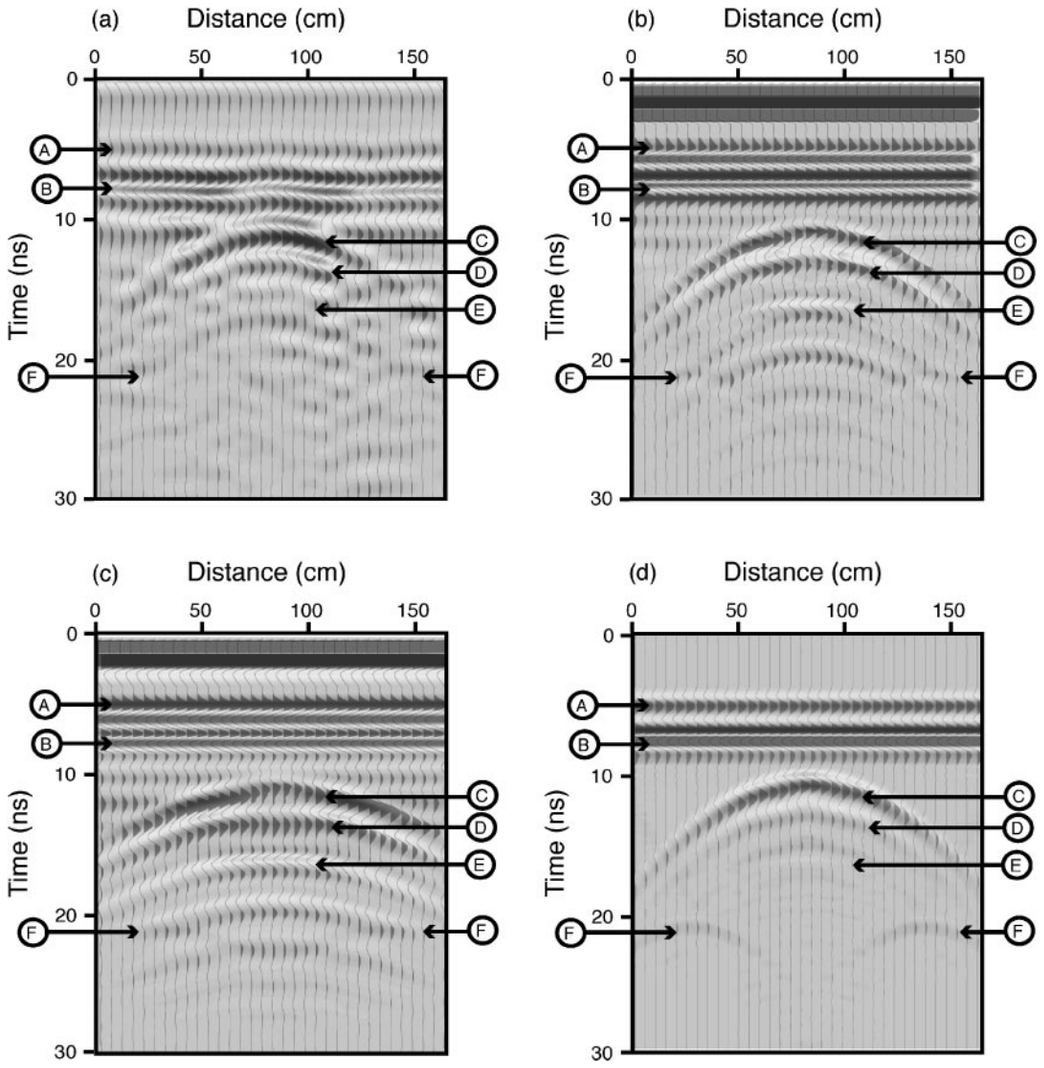

Figure 4. Recorded data (a), monostatic simulation (b), plane-wave simulation (c), and exploding-reflector simulation (d). The monostatic simulation consists of 33 computations. The reflection events are: (A) cement/gravel interface, (B) gravel/clayey soil interface, (C) clayey soil/brick interface, (D) brick/air interface, (E) air/water interface, and (F) clayey soil/brick interface (sides of the tomb).

The radargrams are computed in the space-time domain. We assume propagation in the (x, z)-plane, and that the material properties and source characteristics are constant with respect to the y-coordinate. Let us denote by $\mathcal{E}$ and $\mathcal{H}$ and $\mathcal{J}$ the corresponding time-domain electric and magnetic fields and source, and for convenience, the medium properties are indicated by the same symbols, in both the time and the frequency domains. Under these conditions, $\mathcal{E}_x$, $\mathcal{E}_z$ and $\mathcal{H}_y$ are decoupled from $\mathcal{E}_y$, $\mathcal{H}_x$ and $\mathcal{H}_z$, and the second set of components obeys the TE wave differential equations:

$$\begin{aligned} \frac{\partial \mathcal{H}_x}{\partial z} - \frac{\partial \mathcal{H}_z}{\partial x} &= \epsilon \frac{\partial \mathcal{E}_y}{\partial t} + \sigma \mathcal{E}_y + \mathcal{J}_y \\ \frac{\partial \mathcal{E}_y}{\partial z} &= \mu \frac{\partial \mathcal{H}_x}{\partial t} \\ -\frac{\partial \mathcal{E}_y}{\partial x} &= \mu \frac{\partial \mathcal{H}_z}{\partial t}. \end{aligned} \tag{A-3}$$

The numerical solver used here consists of the pseudospectral Fourier method for computing the spatial derivatives, and a Runge-Kutta method for time integration (Carcione, 1996a, b).

REFERENCES

Baysal, E., Kosloff, D. D., and Sherwood, J. W. C., 1983, Reverse time migration: Geophysics, **48**, 1514–1524.
——— 1984, A two-way nonreflecting wave equation: Geophysics, **49**, 132–141.
Berenguer, J. P., 1994, A perfectly matched layer for the absorption of electromagnetic waves: Journal of Computational Physics, **114**, 185–200.
Bevan, B. W., 1991, The search for graves: Geophysics, **56**, 1310–1319.
Brizzolari, E., Ermolli, F., Orlando, L., Piro, S., and Versino, L., 1992, Integrated geophysical methods in archeological surveys: Journal of Applied Geophysics, **29**, 47–55.
Carcione, J. M., 1996a, Ground radar simulation for archeological applications: Geophysical Prospecting, **44**, 871–888.
——— 1996b, Ground penetrating radar: Wave theory and numerical simulation in lossy anisotropic media: Geophysics, **61**, 1664–1677.

Carcione, J. M., Böhm, G., and Marchetti, A., 1994, Simulation of a CMP seismic section: Journal of Seismic Exploration, **3**, 381–396.
Carcione, J. M., and Cavallini, F., 1995, On the acoustic-electromagnetic analogy: Wave Motion, **21**, 149–162.
Chew, W. C., 1990, Waves and fields in inhomogeneous media, Van Nostrand Reinhold.
Daniels, D. J., 1996, Surface-penetrating radar: Institution of Electrical Engineers.
Imai, T., Sakayama, T., and Kanemori, T., 1987, Use of ground-penetrating radar and resistivity surveys for archeological investigations: Geophysics, **52**, 137–150.
Jol, H. M., Broshi, M., Eshel, H., Freund, R. A., Shroder, Jr., J. F., Reeder, P., and Dubay, R., 2002, GPR investigations at Qumran, Israel: Site of the Dead Sea Scrolls discovery, *in* S. K. Koppenjan and H. Lee, eds., Ninth International Conference on Ground Penetrating Radar, 91–95.
Loewenthal, D., Lu, L., Roberson, R., and Sherwood, J. W. C., 1976, The wave equation applied to migration: Geophysical Prospecting, **24**, 380–399.
Neumann, P., 1973, Divergence effects in a layered earth: Geophysics, **38**, 481–488.
Pérez Gracia, V., Canas, J. A., Pujades, L. G., Clapés, J., Caselles, O., García, F., and Osorio, R., 2000, GPR survey to confirm the location of ancient structures under the Valencian Cathedral (Spain): Journal of Applied Geophysics, **43**, 167–174.
Pipan, M., Baradello, L., Forte, E., Prizzon, A., and Finetti, I., 1999, 2-D and 3-D processing and interpretation of multi-fold ground penetrating radar data: A case history from an archeological site: Journal of Applied Geophysics, **41**, 271–292.
Spagnolini, U., 1997, Permittivity measurements of multilayered media with monostatic pulse radar: IEEE Transactions on Geoscience and Remote Sensing, **35**, 454–463.
Sternberg, B. K., and McGill, J. W., 1995, Archaeology studies in southern Arizona using ground penetrating radar: Journal of Applied Geophysics, **33**, 209–255.
Stewart, D. C., Anderson, W. L., Grover, T. P., and Labson, V. F., 1994, Shallow subsurface mapping by electromagnetic sounding in the 300 kHz to 30 Mhz: Model studies and prototype system assessment: Geophysics, **59**, 1201–1210.
Stove, G. C., and Addyman, P. V., 1989, Ground probing impulse radar: an experiment in archeological remote sensing at York: Antiquity, **63**, 337–342.
Vaughn, C. J., 1986, Ground-penetrating radar surveys used in archeological investigations: Geophysics, **51**, 595–604.